INTL JOURNAL OF ELECTRONICS AND TELECOMMUNICATIONS, 2026, VOL. 72, NO. 1, PP. 1–7
Manuscript received July 17, 2025; revised February, 2026. doi: 10.24425/ijet.2026.157867

Radar detection of high architectural objects in urban environments – an experimental study

Urszula Libal, Arkadiusz Byndas, Dawid Sysak and Tomasz Karaś

***Abstract*—The increasing presence of unmanned aerial vehicles (UAVs) in urban airspace necessitates reliable detection and classification of tall architectural structures to ensure flight safety and effective collision avoidance. This paper presents an experimental study on radar detection of high-infrastructural objects, such as residential blocks, tall buildings, and similar structures, in a complex urban environment. Using a custom X-band radar system, real-world measurements were performed in a metropolitan area characterized by a diverse array of tall obstacles. The study investigates the detectability of these urban objects. The results demonstrate that even single radar echoes can reliably reveal the presence of tall structures, while averaging methods further enhance detection performance and resolution. The results underscore the strong capability of X-band radar systems for deployment within UAV frameworks for situational awareness and collision avoidance. Their utility is particularly evident in demanding urban landscapes where adverse weather can compromise the effectiveness of optical sensors. The study also discusses practical considerations for radar deployment in city environments, providing valuable insights for the development of robust UAV navigation systems.**

***Keywords*—radar signal processing; UAV situational awareness; collision avoidance; UAV obstacle avoidance; target detection; radar system; X-band radar**

I. INTRODUCTION

MODERN urban landscapes are increasingly characterized by the pervasive presence of tall architectural structures, ranging from iconic skyscrapers to a diverse array of other high-rise objects. While prominent residential and office buildings define urban skylines, city environments also frequently encompass a diverse array of other tall structures. These include various types of communication towers, observation and viewing platforms, industrial chimneys and smokestacks, construction cranes, wind turbines (even when situated within or near urban boundaries), and monuments or statues of considerable height. These structures not only shape the visual identity of cities but also profoundly influence urban planning, navigation, and the propagation of various signals, including those utilized by radar systems and unmanned aerial vehicles (UAVs). Their ubiquitous presence creates inherently complex environments for technologies that rely on line-of-sight and signal clarity [1], such as X-band radar systems employed in UAV navigation and collision avoidance. The rapid proliferation and expanding operational scope of UAVs in urban areas have consequently elevated the reliable detection and avoidance of such obstacles to a critical challenge for ensuring flight safety. The efficacy of conventional obstacle detection techniques, which typically utilize optical or LIDAR sensors, is frequently compromised or entirely negated by adverse atmospheric conditions, including fog, heavy precipitation, or intense sunlight [2].

Radar, as an active sensing modality, offers unique capabilities for detecting and classifying infrastructural objects irrespective of prevailing weather and lighting conditions. Among various radar bands, X-band radars are particularly attractive for urban UAV applications due to their inherent high resolution and demonstrated ability to operate effectively even in the presence of significant environmental interference [3]. This makes them increasingly appealing for integration into advanced navigation and collision avoidance systems.

The primary aim of this work is to present a comprehensive experimental study on the radar detection of high architectural structures within a real-world urban environment. The research focuses specifically on evaluating the effectiveness of detecting and distinguishing various objects, such as buildings, public utility facilities, monuments, and other potentially hazardous objects relevant to UAV safety at lower altitudes. This study systematically collected radar signals in real urban environments to analyze how signal processing methods, such as averaging and filtering, influence detection performance and target characterization. The experimental insights contribute significantly to understanding the effectiveness of selected radar detection algorithms. Moreover, the findings suggest promising avenues for developing robust radar systems tailored for autonomous aerial platforms operating in complex urban airspace. A foundational understanding of radar principles, starting with the radar equation, is crucial for comprehending this detection process and system performance.

II. RADAR EQUATION

The radar equation is a fundamental mathematical model that quantifies the relationship between the power received by a radar system and various parameters intrinsic to both the radar itself and the target being observed [4]. It serves as an indispensable tool for analyzing detection range, signal-to-noise ratio, and overall radar performance. The power received, denoted as P_r, is contingent upon the transmitted power P_t,

U. Libal, A. Byndas, D. Sysak, and T. Karaś are with the Wroclaw University of Science and Technology, Faculty of Electronics, Photonics and Microsystems, Poland (e-mail: urszula.libal@pwr.edu.pl).

the directional gains of the transmitting and receiving antennas (G_t and G_r respectively), the wavelength λ of the transmitted signal, the radar cross section (RCS) of the target σ, the distance (range) to the target R, and the cumulative total system losses L. For a monostatic radar configuration, where the transmitting and receiving antennas are co-located, the classic form of the radar equation is expressed as:

$$P_r = \frac{P_t G_t G_r \lambda^2 \sigma}{(4\pi)^3 R^4 L} \tag{1}$$

In this equation, Pr represents the received power, P_t is the transmitted power, G_t and G_r are the gains of the transmit and receive antennas, λ is the wavelength, σ is the radar cross section of the target, R is the range to the target, and L accounts for all system losses (e.g., atmospheric attenuation, transmission line losses, processing losses). While the radar equation quantifies the power of the received signal, the actual process of detecting targets and extracting information from these weak, often noisy, returns relies on sophisticated signal processing techniques, such as the correlation method.

III. PULSE COMPRESSION METHOD FOR RADAR DETECTION

The pulse compression method [5] represents a foundational and highly effective approach in radar signal processing, particularly for the detection of objects using complex-valued radar echoes. This technique operates by cross-correlating a known reference signal—typically a replica of the transmitted pulse or chirp—with the received signal, which invariably comprises a combination of target echoes and various forms of noise. Both the reference and received signals are represented as complex sequences to fully preserve their amplitude and phase information, which is crucial for accurate target characterization. The cross-correlation function, $r_{xy}[k]$, is mathematically defined as:

$$r_{xy}[k] = \sum_{n=0}^{N-1} x^*[n] \cdot y[n+k], \tag{2}$$

where $x^*[n]$ denotes the complex conjugate of the reference signal, $y[n+k]$ represents the received signal shifted by a lag k, and N is the length of the reference signal. The reference signal $x[n]$ is a linear chirp function given by:

$$x[n] = A \cdot e^{j2\pi\left(f_0 nT + \frac{1}{2N}(f_{\text{end}} - f_0)n^2 T\right)}, \tag{3}$$

where f_0 is the initial chirp frequency [Hz], f_{end} is the final chirp frequency [Hz], T is the sampling period ($T = 1/f_s$), N is the number of samples (signal length), n is the sample index ($0 \leq n \leq N-1$), f_s is the sampling frequency [Hz], and A is the signal amplitude. The presence and precise timing of echoes, which directly correspond to detected objects and their respective ranges, are indicated by distinct peaks in the output of the correlation function. This method significantly improves the signal-to-noise ratio (SNR) by coherently integrating the energy of the known waveform, thereby making it an optimal technique for detecting known signals embedded within additive white Gaussian noise (AWGN). In practical radar systems, the correlation method is widely implemented through the use of a matched filter, which is instrumental for applications such as pulse compression, accurate range estimation, and robust target detection in challenging environments.

IV. RADAR SYSTEM ARCHITECTURE AND EXPERIMENTAL SETTING

A. X-Band Radar System Overview

At the heart of the our in-house developed radar system (named by us as ENAVI) [6] was the set consisting of an FPGA [7] and a Zynq SoC (System on Chip) [8] as key components, which provided the ability to program and switch between different chirp waveforms and bandwidths according to experimental requirements. Additionally, the FPGA handled the initialization and calibration processes for the IQ transceiver, ensuring optimal performance and signal integrity. The processed signals and control data were transferred to a personal computer via a high-speed interface. The PC was responsible for data acquisition, storage and visualization, facilitating efficient monitoring and analysis of radar data.

For the purpose of conducting experiments, the beta version of the ENAVI X-band radar, shown in Fig. 1, was used. This version of the radar has a configuration with a low-power (20 W, 43 dBm) radar sensor.

Fig. 1. A photography of the beta version of custom radar system: ENAVI.

B. Radar Configuration

For the purpose of testing, the radar was set up with these main parameters:

- Frequency Band: X-band,
- Max RF output power: 43 dBm,
- IF output power: from -50 to 0 dBm,
- BB modulation bandwidth: 12 MHz,
- Sampling Frequency: 40 MHz,
- RX LPF: 13 MHz,
- Minimum chirp repetition period: 100 μs,
- Chirp modulation type: linear,
- Chirp duration: from 1 to 3 μs,
- Number of scans within one burst: 4 or 8.

This flexible architecture enabled comprehensive and efficient testing of different radar signal configurations, making

Fig. 2. The situational plan of the experimental setting at Wrocław University of Science and Technology campus at Grunwaldzki Square, where the ENAVI radar was installed (at the balcony of the D-20 building marked as location A), and districts: Dąbie, Sępolno and Biskupin, where the radar antennas were directed to, with indicated all high-rise architectural objects (locations B–H). Side-lobes of radar antenna are directed to $\pm 11^\circ$ and $\pm 22^\circ$. Map source: geoportal.gov.pl. Scale 1:10000.

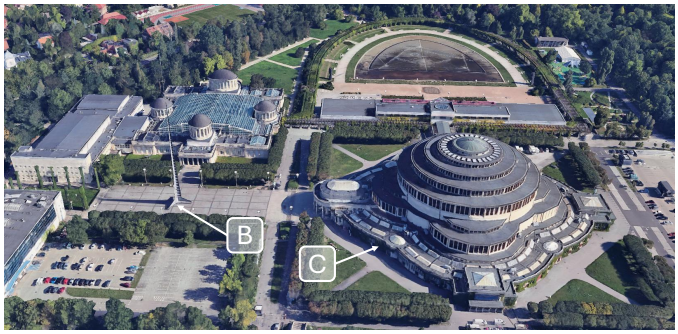

Fig. 3. The 3D visualization of the Iglica (B) and the Centennial Hall (C). Source: Google Map Globe View.

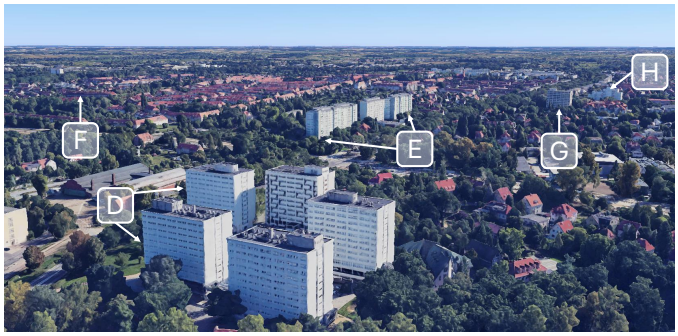

Fig. 4. The 3D visualization of the Wittiga dormitories (D), Kazimierska blocks (E), school at Sępolno (F), Arka dormitory (G) and Raj dormitory (H). Source: Google Map Globe View.

the system highly adaptable to a wide range of research and development applications.

The radar system utilized a linear frequency modulated (chirp) waveform for its measurements. Each burst comprised 80 individual chirps, and a full measurement sequence consisted of 4 and 8 such bursts. The frequency of each chirp varied across a 12 MHz band. Echoes were captured in sequential bursts, with each burst containing a series of four returns, separated by 100-microsecond intervals. The temporal separation between consecutive data packets varied from 100 to 500 milliseconds. The system's pulse repetition frequency (PRF) was set at 10,000 pulses per second. The ENAVI antenna, featuring vertical linear polarization, exhibited a gain of 27 dBi.

C. Outdoor Experimental Settings and Radar Data Acquisition

An ENAVI X-band radar system, configured for vertical-vertical (VV) polarization, was employed to capture radar returns within an urban environment. This specific radar unit is primarily designed for supporting autonomous unmanned aerial vehicle (UAV) operations and enhancing pilot awareness. The primary objective was to collect X-band VV radar signals originating from elevated positions, specifically from the rooftops across Wroclaw, Poland. Consequently, the ENAVI radar was positioned on a rooftop terrace, approximately 45 meters above ground level, for the duration of these tests. Data collection and outdoor trials were conducted from the university's D-20 edifice. From this vantage point, the radar system surveyed the metropolitan expanse, extending its view up to 8 km. These experiments were limited to high-rise buildings in the range of 3 km from the radar. Climatic

TABLE I
LOCATIONS, DISTANCES FROM THE RADAR AND HEIGHTS OF THE HIGH-RISE ARCHITECTURAL LANDMARKS

	Object	Distance [m]	Height [m]	Geographical Coordinates
A	D-20 building (radar location)	0	35.5	51.110202, 17.059828
B	Iglica (spire)	1127	90.3	51.107551, 17.075426
C1	Centennial Hall (front wall)	1239	23.0	51.106960, 17.077339
C2	Centennial Hall (mast in the middle)	1274	42.0	51.106942, 17.077330
D1	Dormitory T-16 at Wittiga Street (first block)	1895	35.0	51.104018, 17.086350
D2	Dormitory T-18 at Wittiga Street (last block)	1994	35.0	51.103601, 17.086361
E1	Buildings at Kazimierska Street (first block)	2249	36.0	51.104568, 17.091329
E2	Buildings at Kazimierska Street (last block)	2500	36.0	51.104078, 17.095283
F	Primary School at Sępolno	2540	22.0	51.109571, 17.095507
G	Dormitory Arka	2785	35.5	51.102131, 17.097379
H	Dormitory Raj	2950	32.0	51.104568, 17.091329

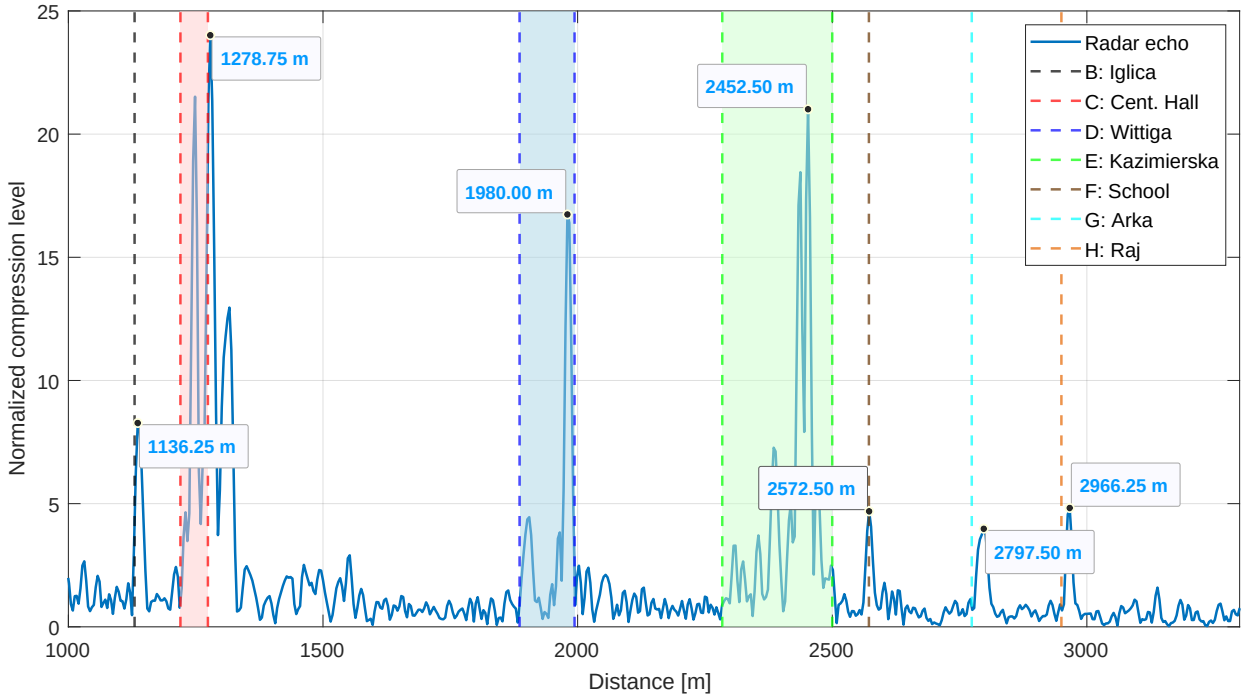

Fig. 5. Radar detection results using a single echo. Detected architectural objects are outlined with dashed lines. Building complexes identified over larger spatial ranges are additionally highlighted with color shading: Centennial Hall (red), Wittiga Street complex (blue), and Kazimierska Street complex (green).

conditions on October 31 were consistent: densely overcast skies with no precipitation.

The map in Fig. 2 illustrates the geographical positions of several prominent architectural features within Wroclaw that were subjects of this investigation, including:

(B) The towering, slender spire known as Iglica,
(C) The expansive Centennial Hall arena,
(D) Student residences situated on Wittiga Street,
(E) Residential complexes located on Kazimierska Street,
(F) The elongated, curved school building in Sępolno,
(G) The Arka dormitory, and
(H) The Raj dormitory.

The details of the architectural objects of interest, which were detected by ENAVI radar, such as their exact geographical coordinates, the distance from the radar (installed at location (A)) and the height, are presented in Table I. Closer look at the detected landmarks are shown in 3D visualizations of the listed buildings in Figs. 3 and 4.

V. RESULTS OF RADAR DETECTION

The imperative for robust radar navigation in UAVs becomes particularly evident when considering operations in challenging environmental conditions, such as low visibility due to rain or fog. Unlike visual-based systems, radar's inherent ability to penetrate these atmospheric obscurants ensures continuous situational awareness and obstacle detection, which is critical for safe and autonomous flight. Furthermore, the radar's pulse characteristics, including its pulse width, are instrumental in achieving precise object detection, even in the presence of significant ground clutter and thermal noise. Our experimental results, which involved averaging across multiple echoes (e.g., four or eight), demonstrated the radar's remarkable capability

to discern targets effectively under such challenging conditions what is presented in Fig. 5.

Intriguingly, our findings indicated that while echo averaging is a common technique for noise reduction, its impact on the clarity of object representation in our specific setup was not substantial. This suggests that even individual radar echoes provided a high-fidelity representation of the observed objects. This performance underscores the potential for radar systems to offer highly reliable and immediate environmental sensing for UAVs, enabling them to navigate complex urban landscapes and adverse weather with enhanced safety and autonomy. Such capabilities are fundamental for expanding the operational envelopes of UAVs beyond clear-sky conditions, unlocking new possibilities for various applications.

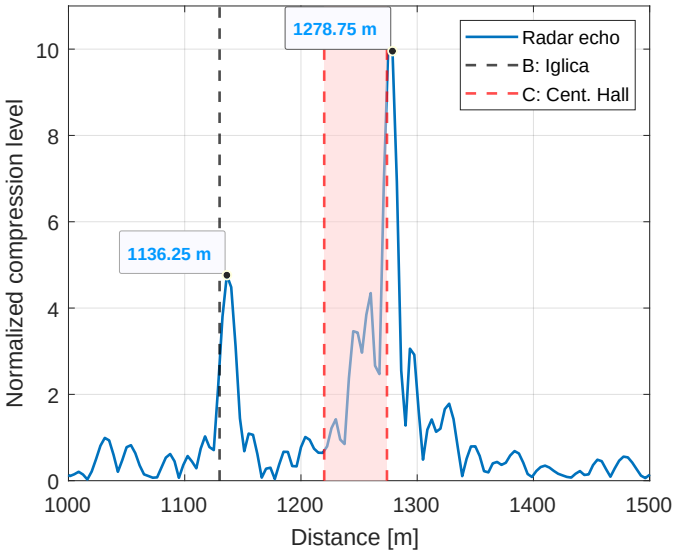

Fig. 6. Detection of the Iglica (the Spire) and the Centennial Hall complex. Dashed lines mark the distances from the radar to the detected architectural structure.

The experimental campaign successfully demonstrated the efficacy of the X-band radar system in discerning and characterizing diverse tall architectural structures within a complex urban environment. Radar measurements taken up to 1500 meters, as depicted in Fig. 6, reveal distinct radar signatures for architectural objects of different sizes and shapes. Specifically, tall, narrow and slender structures like the Iglica (B) exhibit markedly different signal compared to voluminous, spatially expansive buildings such as the Centennial Hall (C). This differentiation underscores the influence of an object's physical dimensions and geometry on its radar cross-section. Despite the inherent challenges posed by metropolitan clutter and the varied geometries of high-rise obstacles, the system consistently captured clear radar returns. A significant finding was the remarkable capability of even a single radar echo to reliably indicate the presence and approximate form of these structures. This inherent robustness suggests a strong signal-to-noise ratio and effective processing, enabling fundamental object detection without extensive signal accumulation.

Further analysis, incorporating advanced averaging methods such as combining four or eight echoes per burst, revealed additional enhancements in detection performance and spatial resolution. While these averaging techniques are typically crucial for mitigating noise and improving target clarity, our observations indicated that the individual echoes already provided a high-fidelity representation of the targets. This implies that for the specific conditions and targets investigated, the radar system inherently offers strong object differentiation, and averaging primarily serves to refine the signal, potentially aiding in finer structural details or in even more severely cluttered environments. The system's ability to penetrate adverse weather conditions, as evidenced by successful data acquisition during heavy overcast, further underscores its advantage over optical sensors in maintaining consistent situational awareness.

Laboratory measurements of the probability of detection for the experimentally estimated false alarm rate at the level of 1.5% is presented in Fig. 7. We can observe the expected fact that for the higher noise levels, the probability of correct detection achieved lower rates.

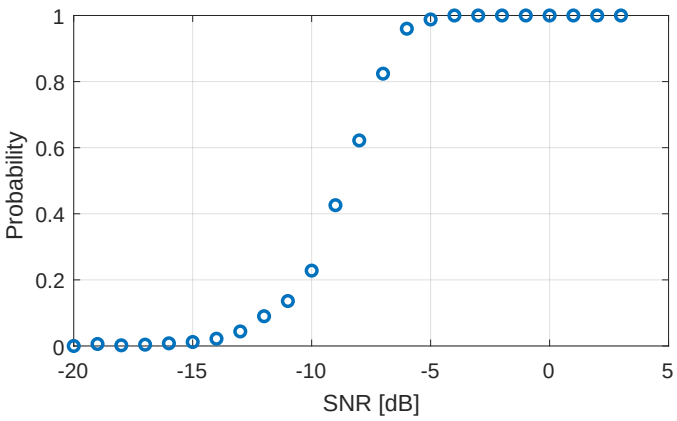

Fig. 7. Estimated detection probability based on radar echoes. Each data point represents the averaged results from 500 measurements at a given SNR level.

The analysis of individual radar echoes, particularly those obtained from the Iglica structure, provides crucial insights into the stability of the received signals. Fig. 8 and Table II present the normalized amplitude and phase values for eight consecutive radar echoes, derived using a correlation method. These data reveal a remarkable consistency in both amplitude and phase across the recorded echoes. The normalized amplitude values, ranging from approximately 4.35 to 4.94, exhibit minimal variance, indicating that the radar returns from the target are highly stable in terms of their power. This suggests a consistent target signature and robust signal reception.

Similarly, the phase values, spanning a narrow range from -0.53 to -0.66 radians, demonstrate excellent phase stability. Such consistency is particularly significant for advanced radar processing techniques that rely on coherent integration, as it minimizes phase noise and allows for more accurate target localization and characterization. The high degree of amplitude and phase stability observed across these individual echoes reinforces the earlier finding that even single radar echoes can provide reliable representations of detected objects. This inherent stability contributes to the system's ability to effectively discern targets even without extensive averaging, as each echo

carries a consistent and strong signature of the illuminated object.

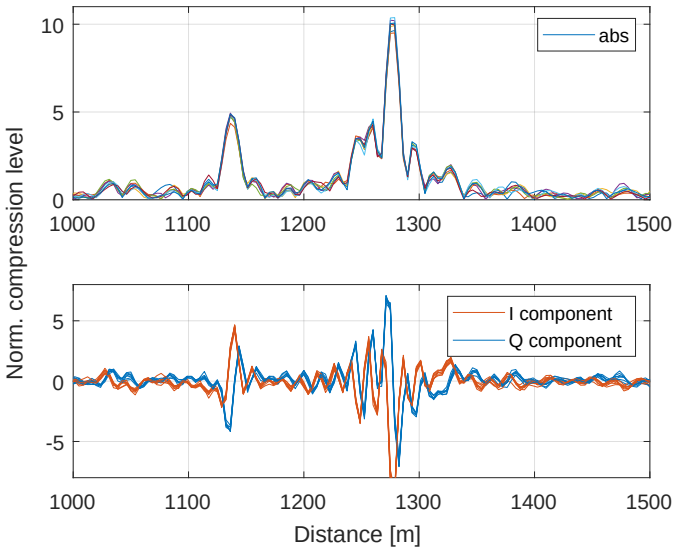

Fig. 8. Amplitude and phase stability of exemplary eight radar echoes, obtained by pulse compression method, for the distance range from 1000 to 1500 m, including the Iglica (B) and the Centennial Hall (C).

TABLE II
AMPLITUDE AND PHASE OF EXEMPLARY EIGHT RECEIVED ECHOES AT THE DISTANCE 1136.25 M – THE ECHO PEAK FOR THE IGLICA (B)

Echo No.	Normalized Amplitude	Phase [rad]
1	4.76	-0.59
2	4.35	-0.57
3	4.82	-0.53
4	4.94	-0.61
5	4.75	-0.66
6	4.78	-0.64
7	4.84	-0.53
8	4.89	-0.60

The stability observed in these fundamental signal parameters underscores the quality of the radar system's performance in an urban environment. It implies that the propagation path and the target's reflective properties remained consistent during the brief measurement period of these eight echoes. This characteristic is highly beneficial for real-time applications such as UAV navigation and collision avoidance, where rapid and accurate target information is paramount. The ability to extract reliable information from individual or very few echoes reduces processing latency and computational load, making the system more agile and responsive in dynamic urban airspaces.

VI. RADAR STABILITY DISCUSSION

Stability is a fundamental requirement for UAV-mounted radar systems, especially in complex urban environments. The reliability of detection, tracking, and measurement accuracy depends on a multitude of parameters, both technical and environmental, that can influence radar performance.

A. Key Parameters Affecting Radar Stability

The consistent and accurate operation of a radar system, particularly for critical applications like UAV navigation, hinges on several key parameters [4], [9]:

- **Phase and Amplitude Stability:** These are critical for precise radar measurements. Phase stability ensures accurate distance and velocity determinations, as phase fluctuations can introduce significant errors in Doppler-based motion detection and degrade overall radar resolution. Amplitude stability, on the other hand, guarantees repeatable and reliable measurements of reflected signal strength. This is essential for robust object classification and the reliable detection of weak targets, as variations in amplitude can lead to an increase in false alarms or missed detections. Our experimental results, as presented in Figure 2 and Table 1, highlight the excellent amplitude and phase stability observed in the received echoes from the Iglica structure, demonstrating the system's inherent consistency in signal generation and reception.
- **Reference Oscillator Quality:** The quality of the radar's internal reference oscillator is paramount. Frequency drift and phase noise originating from this component can directly reduce the accuracy of measurements and significantly diminish radar sensitivity, impacting the system's ability to detect subtle target returns.
- **Mechanical and Environmental Stability:** Radar systems, especially those mounted on dynamic platforms like UAVs, are susceptible to mechanical and environmental influences. Vibrations and platform motion directly affect the stability of received signals, potentially introducing spurious phase shifts and amplitude variations. Furthermore, changes in ambient temperature and humidity can impact the performance of electronic components, leading to phase and amplitude drift. Even minor power supply fluctuations may introduce signal disturbances, compromising data integrity.
- **Propagation Conditions:** The medium through which radar signals propagate significantly influences stability. Electromagnetic interference (EMI) from external sources, such as cellular networks or other radar systems, can cause disruptive interference. In urban environments, pervasive clutter, including reflections from buildings and other structures, leads to multipath effects and signal attenuation, which can complicate target detection and tracking. Additionally, atmospheric phenomena like rain, fog, or snow directly influence signal attenuation and scattering, impacting the overall signal-to-noise ratio.
- **System Calibration and Signal Processing:** Regular system calibration is essential to compensate for inherent changes in antenna and signal path characteristics over time. Complementary to this, advanced filtering algorithms are crucial for mitigating the adverse effects of clutter and inherent signal instability, ensuring that genuine target returns are accurately extracted from noisy backgrounds.
- **Sensor Fusion:** Integrating radar data with information from other onboard sensors, such as Inertial Measurement

Units (IMU) and Global Positioning Systems (GPS), allows for the correction of errors that may arise from temporary instability or external signal interference. This multi-sensor approach enhances the overall robustness and reliability of the navigation solution.

- **Adaptive Control:** The implementation of adaptive control mechanisms, enabling real-time adjustment of radar power and beam direction, can significantly improve detection stability in rapidly changing environments. This allows the radar to dynamically optimize its performance based on prevailing conditions and target characteristics.

B. Importance for UAV Applications

High phase and amplitude stability are essential for effective detection, tracking, and classification of objects in urban settings, directly enabling several critical capabilities for UAV applications. Firstly, such stability leads to increased immunity to false alarms caused by urban clutter. By maintaining consistent signal characteristics from true targets, the radar system can more reliably differentiate them from transient and spurious reflections, thereby reducing navigational errors and enhancing operational safety.

Secondly, high signal stability facilitates precise discrimination between moving and stationary objects. This is crucial for UAVs operating in dynamic environments, allowing them to accurately identify and track other airborne vehicles, ground traffic, or static obstacles. The ability to discern motion with high fidelity is fundamental for collision avoidance algorithms and for maintaining a comprehensive understanding of the surrounding airspace.

Finally, the maintenance of high measurement resolution, even despite strong interference, is directly supported by robust phase and amplitude stability. In signal-dense urban environments, where various electromagnetic sources can introduce noise, a stable radar system ensures that its inherent resolution capabilities are not compromised. This enables UAVs to generate detailed environmental maps, precisely identify the contours of buildings, and accurately locate potential landing zones or hazards, all of which are paramount for autonomous navigation and mission success in complex urban airspaces.

VII. CONCLUSIONS

The experimental study presented herein provides compelling evidence for the critical role of X-band radar systems in advancing UAV navigation and collision avoidance, particularly within challenging urban environments. Our results demonstrate the remarkable capacity of the custom ENAVI radar to reliably detect and distinguish tall urban infrastructure. A key finding was that even single radar echoes can reliably reveal the presence of these structures, underscoring the system's inherent robustness and signal integrity. This capability, coupled with the observed high amplitude and phase stability of the radar returns, positions X-band radar as an indispensable sensor for safe UAV operations.

The necessity for robust radar navigation for UAVs becomes especially apparent when considering operations in adverse weather conditions, such as low visibility due to rain, fog, or heavy overcast. Unlike optical or LIDAR-based systems, radar's ability to penetrate these atmospheric obscurants ensures continuous situational awareness and obstacle detection, which is paramount for flight safety and effective collision avoidance. Our findings indicated that while echo averaging (e.g., across four or eight echoes) can further refine detection performance and resolution, its impact on the clarity of object representation was not substantial in our specific setup, suggesting that individual echoes already provide a high-fidelity representation of the targets.

Ultimately, the independence of X-band radar from visual conditions, coupled with its resilience to clutter and noise, directly addresses critical safety concerns for autonomous flight in complex city environments. The insights gained from this study, particularly regarding the effective performance of single echoes and the importance of signal stability, provide valuable guidance for optimizing radar deployment and signal processing strategies. This work paves the way for the development of more robust, adaptable, and safer UAV platforms capable of operating reliably and autonomously in the increasingly crowded and challenging urban airspace.

ACKNOWLEDGMENT

The authors would like to thank EuroTech Ltd. of Mielec, Poland, for their assistance during radar echo recording. The authors are grateful for the inspiration and cooperation with Mr. Grzegorz Jaromi, Prof. Paweł Kabacik and acknowledge the support provided by the R&D Group on Onboard Telecommunication Electronics for Spacecraft and Transportation at Wroclaw University of Science and Technology, Poland.

REFERENCES

[1] J. N. Yasin, S. A. S. Mohamed, M.-H. Haghbayan, J. Heikkonen, H. Tenhunen, and J. Plosila, "Unmanned aerial vehicles (uavs): Collision avoidance systems and approaches," *IEEE Access*, vol. 8, pp. 105 139–105 155, 2020. [Online]. Available: https://doi.org/10.1109/ACCESS.2020.3000064

[2] Y. Zhang, A. Carballo, H. Yang, and K. Takeda, "Perception and sensing for autonomous vehicles under adverse weather conditions: A survey," *ISPRS Journal of Photogrammetry and Remote Sensing*, vol. 196, pp. 146–177, 2023. [Online]. Available: https://doi.org/10.1016/j.isprsjprs.2022.12.021

[3] A. Moses, M. J. Rutherford, M. Kontitsis, and K. P. Valavanis, "Uav-borne x-band radar for collision avoidance," *Robotica*, vol. 32, no. 1, p. 18, 2014. [Online]. Available: https://doi.org/10.1017/S0263574713000659

[4] M. I. Skolnik, *Introduction to Radar Systems*, 3rd ed. New York: McGraw-Hill, 2001.

[5] M. R. Ducoff and B. W. Tietjen, "Pulse compression radar," in *Radar Handbook*, 3rd ed., M. I. Skolnik, Ed. New York: McGraw-Hill, 2008, ch. 8.

[6] G. Jaromi, P. Kabacik, D. Sysak, and R. Makowski, "Structure and software elements of enavi radar for large drones," in *2021 28th International Conference on Mixed Design of Integrated Circuits and System*, 2021, pp. 249–253. [Online]. Available: https://doi.org/10.23919/MIXDES52406.2021.9497600

[7] AMD Xilinx, "7 series fpgas data sheet: Overview," Online, dS180 (v2.6.1), September 8, 2020. [Online]. Available: https://docs.amd.com/v/u/en-US/ds180_7Series_Overview

[8] AMD, "Zynq-7000 soc data sheet: Overview," Online, dS190 (v1.11.1), 2 July 2018. [Online]. Available: https://docs.amd.com/v/u/en-US/ds190-Zynq-7000-Overview

[9] D. Leeson and G. Johnson, "Short-term stability for a doppler radar: Requirements, measurements, and techniques," *Proceedings of the IEEE*, vol. 54, no. 2, pp. 244–248, 1966. [Online]. Available: https://doi.org/10.1109/PROC.1966.4637